MULTI-PATCHES IRIS BASED PERSON AUTHENTICATION SYSTEM USING PARTICLE SWARM OPTIMIZATION AND FUZZY C-MEANS CLUSTERING

Shekar B. H.[a], Sharada S. Bhat[b*]

[a] Mangalore University, Mangalore, Karnataka India - (bhshekar@gmail.com)
[b] Government Arts and Science College, Karwar, Karnataka, India - (sharadasbhat@gmail.com)

Commission II, WG II/10

KEY WORDS: Particle swarm optimization, Fuzzy c-means, Taylor's series expansion, weighted mean Hamming distance, Iris recognition system

ABSTRACT:

Locating the boundary parameters of pupil and iris and segmenting the noise free iris portion are the most challenging phases of an automated iris recognition system. In this paper, we have presented person authentication frame work which uses particle swarm optimization (PSO) to locate iris region and circular hough transform (CHT) to device the boundary parameters. To undermine the effect of the noise presented in the segmented iris region we have divided the candidate region into N patches and used Fuzzy c-means clustering (FCM) to classify the patches into best iris region and not so best iris region (noisy region) based on the probability density function of each patch. Weighted mean Hammimng distance is adopted to find the dissimilarity score between the two candidate irises. We have used Log-Gabor, Riesz and Taylor's series expansion (TSE) filters and combinations of these three for iris feature extraction. To justify the feasibility of the proposed method, we experimented on the three publicly available data sets IITD, MMU v-2 and CASIA v-4 distance.

1. INTRODUCTION

Being one of the favourites of all biometric traits, iris recognition system is emerged as the best human authentication system. However, it is needed to develop a robust iris recognition system for authentication as well as identification. Eye images taken with visible wavelength (VW) or near infra-red (NIR) camera may include images in which, the difference between the iris and adjacent non-iris region is not clearly distinguishable because of bad illumination, on-move or at-a-distance photography. Also, off-angled and tilted eye images made it difficult to accurately localize the iris and pupil region. After locating the position of the iris, segmenting the candidate iris region is even more complicated and time consuming task. Because, the iris region would normally occluded by eye lids, eye lashes, reflections of light and spectacles. Since, accuracy and speed of iris recognition system highly depend on efficient localization and segmentation process, large number of researchers are working on this issue.

Existing segmentation methods localize the pupillar and limbic boundaries first, and then apply occlusion removal techniques. Several curve fitting techniques are proposed in the literature for occlusion removal. Since both VW and NIR imaging produce degraded and noisy images, occlusion removal is challenging and time consuming task in both authentication and identification scenarios. Moreover, located iris region may not be circular in shape. The irises with irregular shape and occlusion will result into a drastic low recognition rate. In this paper, we have proposed a novel and robust occlusion removal strategy for the degraded, noisy irises.

We have developed an iris authentication frame work which involves the following steps:

1 The iris region is segmented from the input eye image using particle swarm optimization (PSO) and then the pupil and limbic boundary parameters are located using circular hough transform (CHT).

2 Segmented iris region comprises of eyelids, eye lashes, reflection of light and part of adjacent non-iris region (because of non-circular shape). To deal with this issue a novel occlusion removal strategy is applied. Segmented iris region is divided into N patches using tracks and sectors. Unsupervised Fuzzy c-means clustering (FCM) method is applied to classify them into k clusters based on the probability density function of each patch. Each patch is assigned with a weight based on the clustering output and the ground truth of the iris region.

3 Combination of Log-Gabor, Riesz and TSE filters are used to extract the features of each patch and each patch is encoded into binary iris code using Daugman's phase encoding technique. Weighted mean Hamming distance (WMHD) is used to find the dissimilarity scores between the two irises.

We have experimented this method on three publicly available databases, IIT Delhi, MMU v-2 and CASIA v-4 distance and obtained improved recognition rates.

The remainder of the paper is organised as follows: Section 2 summarises the related work, in Section 3 we have detailed the proposed iris authentication frame work, Section 4 comprises of details of experiments and discussions and Section 5 concludes the paper.

2. RELATED WORK

The state-of-art iris segmentation methods can be categorised into two types. First category locates pupil and iris boundaries

---

*Corresponding author

based on the edge information (boundary based methods) and the second category segments the candidate iris region based on the pixel information (pixel-based methods) (Liu et al., 2016). The first boundary-based technique is the integro-differential operator (IDO) introduced by Daugman (Daugman, 1993), and the second one is hough transform (HT) which is first used by Wildes (Wildes, 1997). Various forms of IDO and HT (Wildes, 1997, Zuo et al., 2006, Liu et al., 2005, Jan et al., 2013, Tan et al., 2010) are proposed in the literature. Apart from these two techniques, other boundary based methods found in the literature are, active shape models (Abhyankar and Schuckers, 2006), binary morphology and image statistics (Kennell et al., 2006), adaptive binarisation (Basit and Javed, 2007), Adaboost cascading and elastic model (He et al., 2009), Geodesic active counter (Shah and Ross, 2009), and eyeball model (Baek et al., 2013).

Pixel based methods have used the information such as color, intensity variation and texture of the iris to extract the discriminative appearance feature of a pixel from the neighbourhood pixels (Liu et al., 2016). Proenca and Alexandre (Proença and Alexandre, 2006) have introduced unsupervised clustering techniques, Jeong et al. (Jeong et al., 2010) have used Adaboost eye detection and color segmentation, intelligent random sample consensus iris segmentation on four spectral images is proposed by Chou et al. (Chou et al., 2010) and clustering based coarse eye localization and integro-differential constellation are used by Tan et al. (Tan et al., 2010). Neural network classification is introduced by Proenca (Proenca, 2010) and Li et al. (Li et al., 2010) have used K-means clustering. Quality filters for down sampling is proposed by Du et al. (Du et al., 2011) and Gaussian Mixture Model have been utilised by Li and Savvides (Li and Savvides, 2013). Sahmoud and Abuhaiba (Sahmoud and Abuhaiba, 2013) have used K-means clustering and circular HT and Tan and Kumar (Tan and Kumar, 2014) have proposed Zernike moments to extract the iris pixel information. Recently, Gangwar et al. (Gangwar et al., 2016) have proposed a boundary based course-to-fine strategy for iris localization and Liu et al. (Liu et al., 2016) have proposed iris segmentation models using convolutional neural network. We have proposed a segmentation strategy which exploits both, the pixel information and position with respect to the pixels in the neighbourhood and the geometry of the iris region.

Particle swarm optimisation (PSO) is a bioinspired theory which is first introduced by Kennedy and Eberhart (Eberhart et al., 1995) and has been applied to image segmentation problem by several researchers. Omran et al. (Omran et al., 2002) have introduced PSO for image classification and then used dynamic clustering PSO (Omran et al., 2006) for image segmentation. Chandar et al. have used a PSO variant adapting social and momentum components of the velocity for particle move updates (Chander et al., 2011). A simple modified PSO is proposed by Lee et al. (Lee et al., 2012) to extract both low-level features and high-level image semantics from the color image. Tillet et al. (Tillett et al., 2005) have introduced Darwinien PSO, Ghamisi et al. (Ghamisi et al., 2014) have devised fractional-order Darwinien PSO and these techniques are evaluated on medical images (Ryalat et al., 2016). In the biometrics domain, Parez et al. have used PSO to generate the templates for face and iris localization (Perez et al., 2010) and Chen and Chu have combined probabilistic neural network and PSO to design an optimized classifier model for iris recognition (Chen and Chu, 2009). Inspired by these researches, we have used PSO for segmentation as PSO utilizes localized pixel information as well as global features of iris.

The technique of region-wise feature extraction is previously used by the researchers at the classification stage. Chen et al. (Chen et al., 2006) and Proenca and Alexandre (Proenca and Alexandre, 2007) have proposed the technique of dividing the unwrapped candidate iris into N divisions and obtained the multiple signatures for classification. A modified version of it has been used in (Barpanda et al., 2015), and in (Bastys et al., 2011) and (Pillai et al., 2011) authors have also utilized sector divisions of iris region for noisy and uncooperative iris recognition.

3. PROPOSED IRIS AUTHENTICATION FRAME WORK

An overview of the proposed frame work is shown in Figure 1. Input eye image is preprocessed by smoothing, gamma correction and histogram equalization. We have utilised the pixel information to cluster the input eye image into iris and non-iris regions. The rationale behind using PSO clustering technique are: 1. it has been introduced as a best method for the optimization of continuous nonlinear functions (Eberhart et al., 1995), 2. it has been proved better performing than K-means clustering (Omran et al., 2002, Ganta et al., 2012), 3. in case of biometrics, it is used as a best localization tool for face and iris recognition (Perez et al., 2010), and 4. coarse iris localization needs both local and global optimization and PSO does it simultaneously.
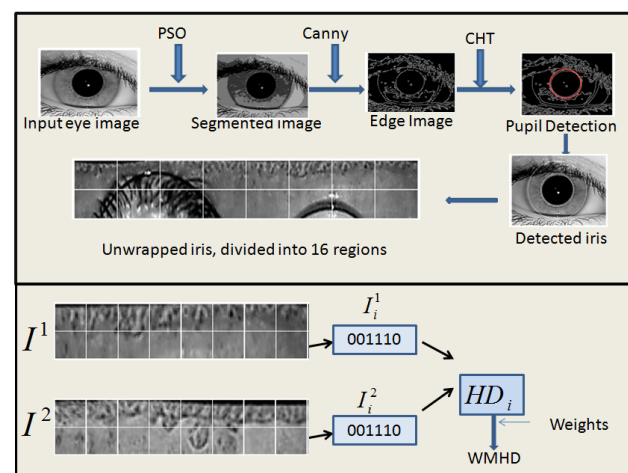

Figure 1. The proposed Iris Authentication frame work

3.1 Particle Swarm Optimisation

The PSO approach automatically determines the optimum number of clusters in a given image and simultaneously clusters the data set with minimal user interference (Omran et al., 2006). It consists of a group of pixels in an image that collectively move in the neighbourhood in search of the global optimum (Ghamisi et al., 2014). Like any other genetic algorithm (GA), PSO is initialized with a population of random solutions. However, unlike GA, here potential solutions, called as particles, are assigned with some randomized velocities (Shi et al., 2001). Each particle is treated as a point in a d-dimensional space (problem space). The ith particle (i^{th} position) is represented as $x_i = (x_{i1}, x_{i2}, ..., x_{id})$. Each particle keeps track of its best previous position, called $pbest$, which is the position that gives the optimum value (best fitness) for the objective function and is represented as $p_i = (p_{i1}, p_{i2}, ..., p_{id})$. Each particle also keeps track of best fitness value it has achieved so far, called $pbest$ value. The

over all best fitness value and its position are also tracked and are called $gbest$ value and $gbest$ position. $gbest$ position is represented by $p_g = (p_{g1}, p_{g2}, ..., p_{gd})$. Objective function is a predefined fitness function of d variables related to the problem to be solved. Particles are initially associated with some random offset values called as velocities, represented as $v_i = (v_{i1}, v_{i2}, ..., v_{id})$. The strategy of PSO concept is, at each step changing the velocity of each particle, i.e. accelerating the particle, towards its $pbest$ and $gbest$ position (Shi and Eberhart, 1998). The velocity and position of the particle are changed using the following equations:

$$v_{ij} = w*v_{ij} + c1*rand()*(p_{ij}-x_{ij}) + c2*Rand()*(p_{gj}-x_{ij}) \tag{1}$$

$$x_{ij} = x_{ij} + v_{ij} \tag{2}$$

where $j \in \{1, 2, ..., d\}$, $c1$ and $c2$ are positive constants, rand() and Rand() are two random functions with the range [0,1] and w is weight factor. The current fitness value of the particle is compared with its $pbest$ value. If the current value is better than the particle's $pbest$ then current position is set as $pbest$ position and the current value is set as $pbest$ value. Current value is also compared with the $gbest$ value and if it is better than $gbest$ then $gbest$ value and $gbest$ position are reset to current value and current position respectively. This process is continued until a predefined good fitness value is met. The parameters $c1$ and $c2$ are called acceleration constants and are both taken as 2.0 for almost all the applications (Shi et al., 2001). Parameter w, also called inertia weight, controls the impact of the previous values of the velocities on the current velocity and hence provides a balance between local and global exploration abilities of the PSO technique (Shi and Eberhart, 1998).

Omran et al. (Omran et al., 2002) have explained how PSO is used in image classification. A swarm is a group of K clusters of the input image. A particle x_i is constructed as $x_i = (c_{i1}, c_{i2}, ..., c_{ij}, ..., c_{iK})$, where each c_{ij} is centroid vector of jth cluster C_{ij}. While d representing the Euclidean distance, the minimum of the inter-class distances between any pair of clusters in the swarm is given by,

$$D_{min}(x_i) = \min_{j \neq k} \{d(c_{ij}, c_{ik})\} \tag{3}$$

Let Z be the matrix that represents the assignment of the pixels to the clusters of particle x_i, i.e. an element z_{ijp} is the pixel in the cluster C_{ij} of the particle x_i. Then maximum of the average intra-class distances of the clusters of the particle x_i is,

$$d_{max}(Z, x_i) = \max_{j=1,2,...,K} \left\{ \sum_{\forall z_p \in C_{ij}} d(z_p, c_{ij})/|C_{ij}| \right\} \tag{4}$$

where $|C_{ij}|$ is the cardinality of the cluster C_{ij}. Objective function F is defined so as to minimise the intra-class distances between the pixels and their cluster means, given by $d_{max}(Z, x_i)$ and to maximise the inter-class distances between the clusters, given by D_{min}.

$$F(x_i, Z) = w1*d_{max}(Z, x_i) + w2*(z_{max} - D_{min}) \tag{5}$$

z_{max} is the maximum pixel value and $w1$ and $w2$ are user defined constants by tuning which, we set the priorities to minimisation of intra-class (candidate iris pixels) differences and maximisation of inter-class (iris and non-iris portion of the eye) differences.

3.2 Multi-patches technique

We have used circular Hough transform to roughly identify the pupil and iris boundary parameters. At this stage, the actual parameters are not identified. Because, the segmented iris is not in exact circular shape. Moreover, the candidate iris region is encompassed with noise and occlusion such as, eye-lids, eye-lashes and photographic reflections. Some surrounding non-iris portion of the iris and some un-useful part of pupil may also be present. This will reduce the percentage of accuracy drastically. In Figure 2, the segmented iris and roughly identified circular structure of the candidate iris region are shown for the eye images taken from the three datasets. It can be seen that candidate iris region is occluded by eyelids, eye lashes and some adjacent non-iris portion.
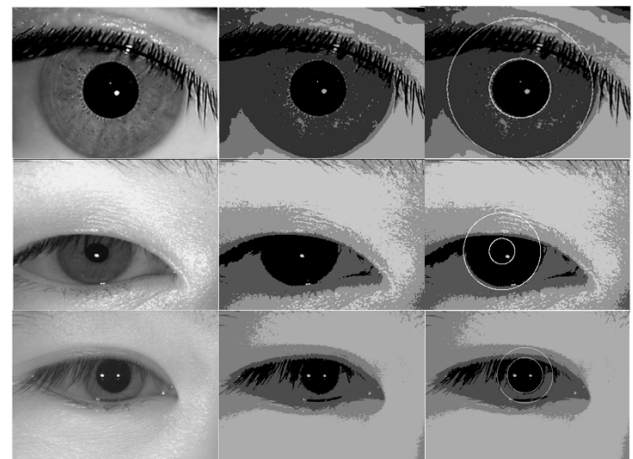

Figure 2. Row-wise : eye images from IIT Delhi, MMU v-2 and CASIA v-4 distance databases. Column-wise : Original eye image, segmented image and roughly identified iris region.

To obtain the portion of the candidate iris region which can be used for further process we have adopted multi-patches technique. The annular iris ring is divided into N patches using m tracks and n sectors. Daugman's doubly dimensionless rubber sheet model (Daugman, 2004) is used to unwrap the iris into uniform sized iris templates. Figure 3 shows an analytical model of annular ring which is divided into 16 patches using two sectors and eight tracks.
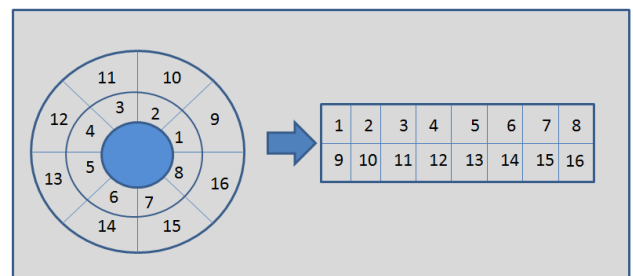

Figure 3. Analytical model of annular iris ring with $m = 2$, $n = 8$ and $N = 16$

The ground truth of the iris image is : the upper and lower region are usually occluded by the eyelids. In (Bastys et al., 2011) the

sectors which contains the upper and lower iris portion are not involved in the feature extraction process. We have not completely omitted these regions. Because, the occluded portion is not uniform among the eye images. It varies from image to image. Hence, we have utilised the statistical properties of the patches to classify them as best iris region and not so best iris region. The probability density function of each patch is separately computed. Based on these properties, patches of iris are grouped into clusters using Fuzzy c-means clustering. The motivation behind using Fuzzy clustering is that the Fuzzy matching is used by (Tsai et al., 2012) to match the two different irises. Properties of iris patches are fuzzy in nature and they possess close statistical relationships. FCM is a well suited tool for such data (Bezdek et al., 1984). We have observed the cluster output and the ground truth of iris and have trained the system to assign the weights to the patches.

3.3 Iris feature extraction filters

We have used Log-Gabor filter given by Masek (Masek and Kovesi, 2003), Riesz filter (Shekar and Bhat, 2015) and Taylor series expansion (TSE) filter (Shekar and Bhat, 2016) and the combinations of these filters and have compared the results. A brief introduction of these filters is given below. Readers can go through the referred papers for details.

3.3.1 Log-Gabor filter Log-Gabor is a Gabor filter which is a Gaussian on logarithmic scale. The frequency output of Log-Gabor is given by the equation,

$$G(f) = Exp\left(\frac{-(log(f/f_0))^2}{2(log(\sigma/f_0))^2}\right) \qquad (6)$$

The filter response of Log-Gabor is encoded into binary bits using Daugman's phase encoding technique (Daugman, 1993). The real and imaginary parts in the filter output are encoded based on their zero crossings. Thus, each pixel is encoded into 2 bit binary code.

3.3.2 Riesz filter Two dimension Riesz kernels are given by,

$$h_x = \frac{1}{2\pi}\frac{x}{\|x\|^3} \;,\;\; h_y = \frac{1}{2\pi}\frac{y}{\|x\|^3} \qquad (7)$$

where $\|.\|$ is the Euclidean norm. The components of first order monogenic Riesz signals $\{h_x f, h_y f\}$ are obtained by convolving the input function $f(x,y)$ with the above kernels. The components of second order monogenic Riesz signals $\{h_{xx} f, h_{xy} f, h_{yy} f\}$ are obtained by convolving the components of the first order signals with the 2D kernels given in equation (7). Each pixel in the input image is encoded into 3 bits binary code by binarising the second order monogenic signals based on the zero crossings.

3.3.3 TSE filter The partial sums of Taylor series expansion (TSE) taking the derivatives along angular axis ($\theta - axis$) and radial axis ($r - axis$) are computed on multiscales.

$$AngularSum = \sum_{n=1}^{N}(\theta - \eta)^n \frac{1}{n!}\frac{\partial^n}{\partial\theta^n}I(\xi,\eta) \qquad (8)$$

$$RadialSum = \sum_{n=1}^{N}(r - \xi)^n \frac{1}{n!}\frac{\partial^n}{\partial r^n}I(\xi,\eta) \qquad (9)$$

where $I(r,\theta)$ is the unwrapped iris template in $r\theta$ space and (ξ,η) is any arbitrary point in the interval of (r,θ). The phase

information at the zero crossings of these signals are further used to encode a pixel into binary bits. $\varepsilon = \theta - \eta$ and $\delta = r - \xi$ are called scale factors and are computed using the following equations:

$$\varepsilon_i = \frac{1}{m}(\theta_{max} - \theta_{min}) * i, \;\; \delta_j = \frac{1}{n}(r_{iris} - r_{pupil}) * j \quad (10)$$

where θ_{min} and θ_{max} are the minimum and maximum values through which θ varies during the unwrapping process and r_{iris} and r_{pupil} are the radii of the iris and pupil regions respectively. Each scale generates 2 binary bits. In our experiments we have taken four different scales to generate 8 bit encoding of the iris pixel.

3.4 Weighted mean Hamming distance (WMHD)

In this section the procedure to find the final dissimilarity score between the two irises is explained. Let I^1 and I^2 be the two unwrapped irises, I_i^1 and I_j^2, $i, j \in \{1, 2, ..., N\}$, be the ith and j^{th} patch of I^1 and I^2 respectively. Each patch is convolved with a filter (LogGabor, Riesz or TSE) and filter output is encoded into binary bits using Daugman's phase encoding technique. Let HD_i be the dissimilarity score between the correspondent patches I_i^1 and I_i^2, calculated using hamming distance. Let w_{1i} and w_{2i}, $i \in \{1, 2, ..., N\}$, be the weights assigned to the patches I_i^1 and I_i^2 respectively. To compute the final set of weights w_i we have experimented the following different strategies.

$$\text{S1. Arithmetic Mean}: w_i = \frac{1}{2}(w_{1i} + w_{2i}) \qquad (11)$$

$$\text{S2. Geometric Mean}: w_i = \sqrt{(w_{1i} * w_{2i})} \qquad (12)$$

$$\text{S3. Maximum Value}: w_i = max\,(w_{1i}, w_{2i}) \qquad (13)$$

$$\text{S4. } w_i = \begin{cases} 0, & \text{if } w_{1i} = 0, w_{2i} = 0 \\ max\,(w_{1i}, w_{2i}), & \text{otherwise} \end{cases} \qquad (14)$$

Final dissimilarity score between the irises I^1 and I^2 is computed using the weighted mean distance given by,

$$HD_{I^1 I^2} = \frac{\sum_{i=1}^{N} w_i * HD_i}{\sum_{i=1}^{N} w_i} \qquad (15)$$

4. EXPERIMENTAL RESULTS

We have conducted the experiments on three benchmark datasets IIT Delhi (*Indian Institute of Technology Delhi Iris Database*, n.d.), MMU v-2 (*Malaysia Multimedia University iris database*, n.d.) and CASIA v-4 distance (*Institute of Automation, Chinese Academy of Sciences.CASIA iris database*, n.d.). IITD database comprises 2240 eyes of 224 persons between the age group 14 to 55 years, containing 176 males and 48 females. This database has deformed noisy eyes with occlusions by eye lids and eye lashes, having 10 eyes of each subject, where, first five are left eyes and next five are right eyes. We have conducted our experiments on 1000 eyes of the first 100 subjects. MMU v-2 database consists of off angled, non cooperative and occluded eyes of 99 subjects, with five left and five right eye images, from which all 99 subjects are involved in our experiments. CASIA v-4 distance is a subset of CASIA v-4 (*Institute of Automation, Chinese Academy of Sciences.CASIA iris database*, n.d.) database which composes of wide varieties of non cooperative and noisy eyes taken at a distance of three meters. This database has 2567 eyes of 142 subjects

Databases	Segmentation Accuracy
IIT Delhi	98.20
MMU v-2	95.66
CASIA v-4 distance	90.50

Table 1. Segmentation accuracy obtained by the proposed method on different databases.

Strategy	Recognition Rate
S1	92.50
S2	98.20
S3	92.50
S4	98.96

Table 2. Recognition rates using different strategies

and each image has dual-eye iris from which patterns of left and right irises can be independently accessed. We have conducted our experiments on 1400 eyes by taking first ten left eyes and ten right eyes of first 70 subjects.

In our experiments we have used the segmentation level as 4.0 in the computation of PSO segmented image. Canny edge detector (with threshold level = 2) is used to get the edge map from the PSO segmented image. The edge map thus obtained is subjected to Hough transform to coarsely locate the centres and radii of pupil and iris. While computing the segmentation accuracy we have manually noted down the correctly segmented irises and segmentation accuracy is computed as the ratio of the number of correctly segmented irises to the total number of eye images taken for the experiment. The percentages of segmentation accuracy obtained on IITD, MMU v-2 and CASIA v-4 distance databases are given in Table 1.

During the experiments we have selected first 20 eye images from each database. The segmented iris is divided into 16 patches using 2 tracks and 8 sectors. These 16 patches are clustered into 5 groups. We have computed the probability density function of each patch and a 2D vector of mean and standard deviation is given as input to FCM. The cluster output and the ground truth of the 16 patches are compared and accordingly weights are assigned as $1, 0.75, 0.5, 0.25, 0.0$ representing, best iris, iris, partially iris, less partially iris and no iris respectively. An example of iris patches and graphical representation of the clustered output is shown in Figure 4.
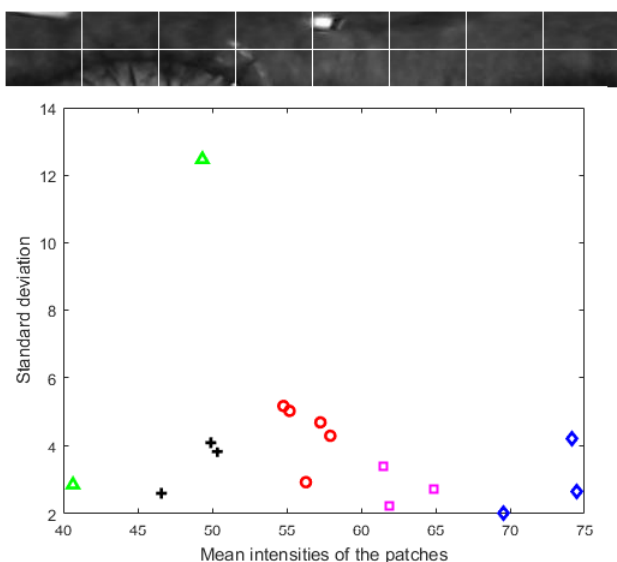
and recognition rates obtained on IITD database taking training to test ratio as 3:2 are presented in Table 2. We have observed that strategies S2 (geometric mean) and S4 have given the good results. We have experimented the proposed segmentation method and multi-patch technique on the IITD, MMU v-2 and CASIA v-4 distance databases using the feature extraction techniques explained in section 3.3. Experiments are conducted using bit level fusion technology given in (Shekar and Bhat, 2015). Recognition rates obtained on the three databases applying the filters Log-Gabor, Riesz and TSE and their combinations are presented in Table 3. To compute WHMD strategy S4 is used and training to test ratio is 3:2. ROC curves of the same experiments are given in Figure 5, 6 and 7.

Method	IITD	MMU v-2	CASIA v-4 dist
Gabor	92.50	85.50	80.00
Riesz	95.00	86.34	82.50
Taylor	97.50	87.00	85.00
Gabor+Riesz	93.33	87.50	85.00
Gabor+Taylor	97.66	90.00	85.00
Riesz+Taylor	98.50	92.33	87.50
Gabor+Riesz+Taylor	98.96	95.67	90.00

Table 3. Recognition rates obtained by different feature extraction methods on the three databases
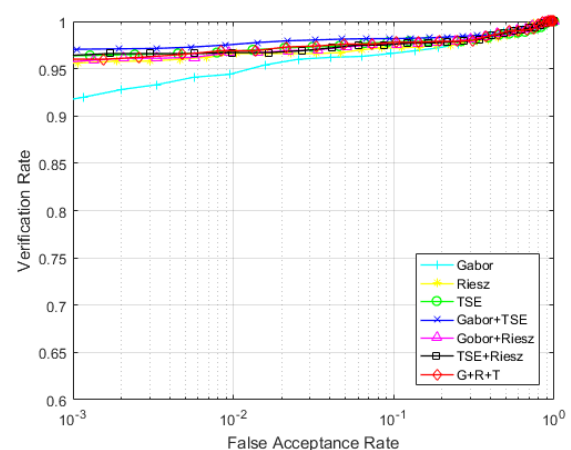

Figure 4. An example of iris patches and graphical representation of the clustered output.

Figure 5. ROC curve obtained on database.

Further, we calculated the dissimilarity score of two irises using WMHD, using the four strategies as explained in the section 3.4

5. CONCLUSION

In this work, we have devised an iris authentication frame work comprising novel iris segmentation and occlusion elimination strategies. Extensive experiments are conducted to justify accuracy of the proposed strategies in authentication scenario. Unlike
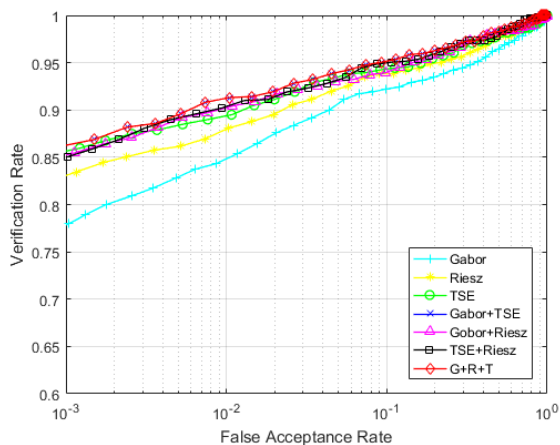
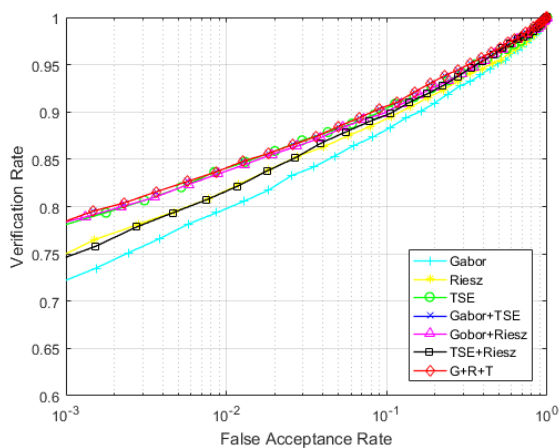Figure 6. ROC curve obtained on MMU v-2 database.

Figure 7. ROC curve obtained on CASIA v-4 distance database.

the existing methods of occlusion removal, proposed strategy is simple and easy to implement. Some of the eye images in the databases are completely degraded (refer Figure 8) and such images are not counted while calculating the segmentation accuracy.

Figure 8. Exanples of degraded eye images.

REFERENCES

Abhyankar, A. and Schuckers, S., 2006. Active shape models for effective iris segmentation. In: *Defense and Security Symposium*, International Society for Optics and Photonics, pp. 62020H–62020H.

Baek, S.-J., Choi, K.-A., Ma, C., Kim, Y.-H. and Ko, S.-J., 2013. Eyeball model-based iris center localization for visible image-based eye-gaze tracking systems. *IEEE Transactions on Consumer Electronics* 59(2), pp. 415–421.

Barpanda, S. S., Majhi, B. and Sa, P. K., 2015. Region based feature extraction from non-cooperative iris images using triplet half-band filter bank. *Optics & Laser Technology* 72, pp. 6–14.

Basit, A. and Javed, M., 2007. Localization of iris in gray scale images using intensity gradient. *Optics and Lasers in Engineering* 45(12), pp. 1107–1114.

Bastys, A., Kranauskas, J. and Krüger, V., 2011. Iris recognition by fusing different representations of multi-scale taylor expansion. *Computer Vision and Image Understanding* 115(6), pp. 804–816.

Bezdek, J. C., Ehrlich, R. and Full, W., 1984. Fcm: The fuzzy c-means clustering algorithm. *Computers & Geosciences* 10(2-3), pp. 191–203.

Chander, A., Chatterjee, A. and Siarry, P., 2011. A new social and momentum component adaptive pso algorithm for image segmentation. *Expert Systems with Applications* 38(5), pp. 4998–5004.

Chen, C.-H. and Chu, C.-T., 2009. High performance iris recognition based on 1-d circular feature extraction and pso–pnn classifier. *Expert Systems with Applications* 36(7), pp. 10351–10356.

Chen, Y., Dass, S. C. and Jain, A. K., 2006. Localized iris image quality using 2-d wavelets. In: *International conference on biometrics*, Springer, pp. 373–381.

Chou, C.-T., Shih, S.-W., Chen, W.-S., Cheng, V. W. and Chen, D.-Y., 2010. Non-orthogonal view iris recognition system. *IEEE Transactions on Circuits and Systems for Video Technology* 20(3), pp. 417–430.

Daugman, J., 2004. How iris recognition works. *IEEE Transactions on circuits and systems for video technology* 14(1), pp. 21–30.

Daugman, J. G., 1993. High confidence visual recognition of persons by a test of statistical independence. *Pattern Analysis and Machine Intelligence, IEEE Transactions on* 15(11), pp. 1148–1161.

Du, Y., Arslanturk, E., Zhou, Z. and Belcher, C., 2011. Video-based noncooperative iris image segmentation. *IEEE Transactions on Systems, Man, and Cybernetics, Part B (Cybernetics)* 41(1), pp. 64–74.

Eberhart, R. C., Kennedy, J. et al., 1995. A new optimizer using particle swarm theory. In: *Proceedings of the sixth international symposium on micro machine and human science*, Vol. 1, New York, NY, pp. 39–43.

Gangwar, A., Joshi, A., Singh, A., Alonso-Fernandez, F. and Bigun, J., 2016. Irisseg: A fast and robust iris segmentation framework for non-ideal iris images. In: *Biometrics (ICB), 2016 International Conference on*, IEEE, pp. 1–8.

Ganta, R. R., Zaheeruddin, S., Baddiri, N. and Rao, R. R., 2012. Particle swarm optimization clustering based level sets for image segmentation. In: *2012 Annual IEEE India Conference (INDICON)*, IEEE, pp. 1053–1056.

Ghamisi, P., Couceiro, M. S., Martins, F. M. and Benediktsson, J. A., 2014. Multilevel image segmentation based on fractional-order darwinian particle swarm optimization. *IEEE Transactions on Geoscience and Remote sensing* 52(5), pp. 2382–2394.

He, Z., Tan, T., Sun, Z. and Qiu, X., 2009. Toward accurate and fast iris segmentation for iris biometrics. *IEEE transactions on pattern analysis and machine intelligence* 31(9), pp. 1670–1684.

Jan, F., Usman, I. and Agha, S., 2013. Reliable iris localization using hough transform, histogram-bisection, and eccentricity. *Signal Processing* 93(1), pp. 230–241.

Jeong, D. S., Hwang, J. W., Kang, B. J., Park, K. R., Won, C. S., Park, D.-K. and Kim, J., 2010. A new iris segmentation method for non-ideal iris images. *Image and vision computing* 28(2), pp. 254–260.

Kennell, L. R., Ives, R. W. and Gaunt, R. M., 2006. Binary morphology and local statistics applied to iris segmentation for recognition. In: *2006 International Conference on Image Processing*, IEEE, pp. 293–296.

Lee, C.-Y., Leou, J.-J. and Hsiao, H.-H., 2012. Saliency-directed color image segmentation using modified particle swarm optimization. *Signal Processing* 92(1), pp. 1–18.

Li, P., Liu, X., Xiao, L. and Song, Q., 2010. Robust and accurate iris segmentation in very noisy iris images. *Image and Vision Computing* 28(2), pp. 246–253.

Li, Y.-H. and Savvides, M., 2013. An automatic iris occlusion estimation method based on high-dimensional density estimation. *IEEE transactions on pattern analysis and machine intelligence* 35(4), pp. 784–796.

Liu, N., Li, H., Zhang, M., Liu, J., Sun, Z. and Tan, T., 2016. Accurate iris segmentation in non-cooperative environments using fully convolutional networks. In: *Biometrics (ICB), 2016 International Conference on*, IEEE, pp. 1–8.

Liu, X., Bowyer, K. W. and Flynn, P. J., 2005. Experiments with an improved iris segmentation algorithm. In: *Fourth IEEE Workshop on Automatic Identification Advanced Technologies (AutoID'05)*, IEEE, pp. 118–123.

Masek, L. and Kovesi, P., 2003. Matlab source code for a biometric identification system based on iris patterns. *The School of Computer Science and Software Engineering, The University of Western Australia.*

Omran, M. G., Salman, A. and Engelbrecht, A. P., 2006. Dynamic clustering using particle swarm optimization with application in image segmentation. *Pattern Analysis and Applications* 8(4), pp. 332–344.

Omran, M., Salman, A. and Engelbrecht, A. P., 2002. Image classification using particle swarm optimization. In: *Proceedings of the 4th Asia-Pacific conference on simulated evolution and learning*, Vol. 1, Singapore, pp. 18–22.

Perez, C. A., Aravena, C. M., Vallejos, J. I., Estevez, P. A. and Held, C. M., 2010. Face and iris localization using templates designed by particle swarm optimization. *Pattern recognition letters* 31(9), pp. 857–868.

Pillai, J. K., Patel, V. M., Chellappa, R. and Ratha, N. K., 2011. Secure and robust iris recognition using random projections and sparse representations. *IEEE Transactions on Pattern Analysis and Machine Intelligence* 33(9), pp. 1877–1893.

Proenca, H., 2010. Iris recognition: On the segmentation of degraded images acquired in the visible wavelength. *IEEE Transactions on Pattern Analysis and Machine Intelligence* 32(8), pp. 1502–1516.

Proença, H. and Alexandre, L. A., 2006. Iris segmentation methodology for non-cooperative recognition. *IEE Proceedings-Vision, Image and Signal Processing* 153(2), pp. 199–205.

Proenca, H. and Alexandre, L. A., 2007. Toward noncooperative iris recognition: a classification approach using multiple signatures. *IEEE Transactions on Pattern Analysis and Machine Intelligence* 29(4), pp. 607–612.

Ryalat, M. H., Emmens, D., Hulse, M., Bell, D., Al-Rahamneh, Z., Laycock, S. and Fisher, M., 2016. Evaluation of particle swarm optimisation for medical image segmentation. In: *International Conference on Systems Science*, Springer, pp. 61–72.

Sahmoud, S. A. and Abuhaiba, I. S., 2013. Efficient iris segmentation method in unconstrained environments. *Pattern Recognition* 46(12), pp. 3174–3185.

Shah, S. and Ross, A., 2009. Iris segmentation using geodesic active contours. *IEEE Transactions on Information Forensics and Security* 4(4), pp. 824–836.

Shekar, B. and Bhat, S. S., 2016. Iris recognition using partial sum of second order taylor series expansion. In: *Proceedings of the Tenth Indian Conference on Computer Vision, Graphics and Image Processing*, ACM, p. 81.

Shekar, B. H. and Bhat, S. S., 2015. Steerable riesz wavelet based approach for iris recognition. In: *2015 3rd IAPR Asian Conference on Pattern Recognition (ACPR)*, IEEE, pp. 431–436.

Shi, Y. and Eberhart, R. C., 1998. Parameter selection in particle swarm optimization. In: *International Conference on Evolutionary Programming*, Springer, pp. 591–600.

Shi, Y. et al., 2001. Particle swarm optimization: developments, applications and resources. In: *evolutionary computation, 2001. Proceedings of the 2001 Congress on*, Vol. 1, IEEE, pp. 81–86.

Tan, C.-W. and Kumar, A., 2014. Accurate iris recognition at a distance using stabilized iris encoding and zernike moments phase features. *IEEE Transactions on Image Processing* 23(9), pp. 3962–3974.

Tan, T., He, Z. and Sun, Z., 2010. Efficient and robust segmentation of noisy iris images for non-cooperative iris recognition. *Image and vision computing* 28(2), pp. 223–230.

Indian Institute of Technology Delhi Iris Database, n.d. http://www.comp.polyu.edu.hk/csajaykr/IITD/database.html.

Institute of Automation, Chinese Academy of Sciences.CASIA iris database, n.d. http://biometrics.idealtest.org/.

Malaysia Multimedia University iris database, n.d. http://pesona.mmu.edu.

Tillett, J., Rao, T., Sahin, F. and Rao, R., 2005. Darwinian particle swarm optimization.

Tsai, C.-C., Lin, H.-Y., Taur, J. and Tao, C.-W., 2012. Iris recognition using possibilistic fuzzy matching on local features. *IEEE Transactions on Systems, Man, and Cybernetics, Part B (Cybernetics)* 42(1), pp. 150–162.

Wildes, R. P., 1997. Iris recognition: an emerging biometric technology. *Proceedings of the IEEE* 85(9), pp. 1348–1363.

Zuo, J., Kalka, N. D. and Schmid, N. A., 2006. A robust iris segmentation procedure for unconstrained subject presentation. In: *2006 Biometrics Symposium: Special Session on Research at the Biometric Consortium Conference*, IEEE, pp. 1–6.